

Mathematical modeling & performance analysis of FSO-based XG-PON using 2D multi-diagonal code

KEHKASHAN A. MEMON^{1,*}, NOORAIN MUKHTIAR¹, FARIDA MEMON¹, ZARTASHA BALOUCH²,
SAIMA SHAIKH³, AQSA YOUSIF SHAIKH⁴

¹Mehran University of Engineering & Technology, Department of Electronics, Pakistan

²Mehran University of Engineering & Technology, Department of Computer System, Pakistan

³Sindh Agricultural University, Department of Information Technology, Pakistan

⁴Ilma University, Department of Software Engineering, Pakistan

In this article, the Next Generation Passive Optical Network architecture is designed, analyzed, and validated using mathematical analysis of two-dimensional Multi-diagonal optical codes and Free Space Optical channel in the last mile. The performance is analytically evaluated under various weather conditions, and it has been observed that the proposed network design is providing promising results for next-generation gigabit traffic of upto 10 Gbps per user. Shot noise, thermal, and atmospheric noise are taken into consideration to analyze the system. This All-Optical system provides BER of 10^{-9} and high SNR in heavy rain to hazy weather, thereby making it reliable for the next generation (XG-PON).

(Received March 14, 2024; accepted August 1, 2024)

Keywords: XG-PON, FSO, 2D Multi-Diagonal Codes, Mathematical Model, SNR, BER

1. Introduction

The increasing prevalence of intelligent and smart devices has generated an escalating requirement for uninterrupted connectivity to almost every conceivable aspect of our lives. This surge in demand is driving the need for rapid data speeds that can effectively accommodate a diverse array of services. In the past, data transmission has been facilitated through various types of connections from dial-up to cellular communication. To understand the technological advancement of this time, it is important to go through the past technologies used for communication. Starting with dial-up connections, reliant on modems, were cost-effective but have now become obsolete due to their extremely slow speed. Broadband, using various channels like coaxial cables and optical fibers, provides high-speed internet for multiple users simultaneously. Digital Subscriber Line (DSL) uses telephone lines, offering constant connectivity with speed ranging from 128 k to 8 Mbps. Cable modems use cable TV lines for remarkably fast internet, reaching speed from 512 k to 20 Mbps. Satellite connectivity serves rural areas, but with noticeable delays, providing a speed range from 512 Kbps to 2 Mbps. Wireless internet avoids cables and relies on radio frequencies with a speed range of 5 Mbps to 20 Mbps. Cellular technology is accessible through cell phones, including 3G with speed around 2 Mbps and 4G around 21 Mbps, while aiming for 100 Mbps. Each technology has played a role in shaping the diverse landscape of contemporary communication.

With the above discussion, it is evident that the mentioned variants of technologies are providing speeds in Mbps. In this high-tech era, we are dealing with the

Internet of Things (IoT) and triple-play services (i.e., high speed internet, television, and telephone network), controlling home appliances from far away with a single click, and enjoying high-definition online video conferencing among other numerous advantages. However, the data rate in Mbps may prove insufficient to leverage these benefits. A network architecture is required, capable of not only meeting the contemporary demands for high data rates but also accommodating future requirements. Two-Dimensional Optical Code Division Multiple Access (OCDMA) and Free Space Optics (FSO) are two potential and advantageous technologies of optical communication. With the addition of 2D-OCDMA codes and FSO, the network infrastructure can support high cardinality with excellent spectral efficiency. This will provide not only higher data rates but also simplicity and uniformity in the network from service provider to last-mile network. The proposed system focuses on OCDMA, 2D codes, FSO, and XG-PON, their background is briefly discussed below.

a. Optical Code Division Multiple Access

OCDMA stands as a technique for enabling multiple accesses. This method permits multiple users to concurrently transmit and receive data via the same optical fiber. It combines the benefits of optical fiber technology with CDMA for rapid communication networks. A unique code is provided to every individual user as shown in Fig. 1, which can be one, two, or even three-dimensional code. In recent times, the OCDMA approach has gained popularity due to its multifaceted features. It can accommodate asynchronous access, handle bursty traffic,

ensure stable transmission, and maintain cost efficiency, rendering it an attractive option [1], [2]. OCDMA surpasses the capabilities of Wavelength Division Multiple (WDM) and showcases unmatched capacity, a fact

substantiated through simulation studies [3]. This emphasizes its potential significance in the realm of communication technology.

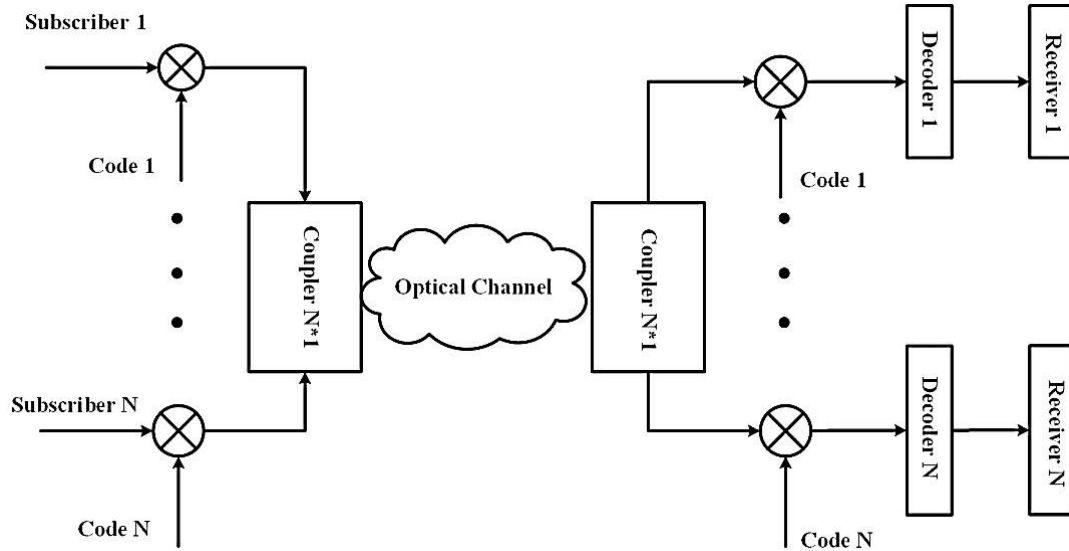


Fig. 1. OCDMA Block Diagram

b. 2D Multi Diagonal code

OCDMA technology involves the selection of choices from several aspects such as the type of optical sources (coherent or incoherent, narrowband or broadband), coding methods (in terms of time or wavelength, amplitude or phase), and detection strategies (coherent or incoherent). The following six main coding technique categories are outlined in [4].

- Pulse phase coding
- Spectral amplitude coding (SAC)
- Spectral phase coding
- Wavelength hopping time spreading coding
- Spatial coding
- Pulse-amplitude coding

The encoder and decoder design are of paramount importance and tailored to the specific application of the OCDMA system. Typically, the structure of the encoder and decoder can be established through the utilization of optical delay lines, methods involving diffraction Gratings, Fiber Bragg Gratings (FBGs), or array waveguide gratings (AWGs). In an OCDMA network, the capacity for accommodating users employing one-dimensional (1-D) incoherent time-domain encoding is quite constrained. This constraint arises due to the relationship between the number of users and the extent of frequency spreading. As the user count increases, the frequency-spreading length also increases, leading to a decrease in data rate for individual users. Consequently, a higher count of network users gives rise to more pronounced instances of Multiple User Interference (MUI) or Multiple Access Interferences (MAI).

In real-world scenarios, the device's Bit Error Rate (BER) rises, and the potential for numerous subscribers to concurrently communicate becomes restricted. To address the limitations of one-dimensional incoherent OCDMA codes, two-dimensional (2-D) codes were introduced. In a broader context, research indicates that incoherent OCDMA systems employing 2-D encoding outperform hybrid systems that combine OCDMA with other multiple-access techniques such as wavelength division multiple access, as demonstrated in [5]. The creation of a 2D code is achievable through various permutations of time, spectral, and spatial dimensions. Extensive exploration has taken place in the realms of 2D spectral/time, spectral/spatial, and spatial/time domains, as extensively investigated by [6]. 2D codes were introduced by merging two distinct approaches (time, wavelength, spatial). This amalgamation of codes led to the creation of two-dimensional codes. For instance, combining 1D-Zero Cross-Correlation (ZCC) and 1D- Multi diagonal (MD) codes resulted in the formation of a 2D-ZCC/MD code for spectral/spatial OCDMA codes, as proposed by [7].

The 2D code methodology employs a code length that is shorter compared to 1D codes, with the aim of optimizing the network's capacity for accommodating numerous subscribers. This is achieved by partitioning the code into two distinct domains. The 2D strategy offers the advantage of mitigating the adverse impacts of MAI and phase-induced intensity noise (PIIN), facilitating the accommodation of multiple active users at elevated data rates, and enhancing spectral efficiency.

The current study was undertaken to deploy a 2D spectral/spatial coding framework for OCDMA, which holds the capability to enhance the overall performance of the OCDMA network. The concept of the 2D-MD code

was elucidated in [8], where the authors utilized 1D-MD codes as detailed in [9] to formulate the 2D code. The primary reason for selecting the 2D-MD code stems from its capacity to effectively eliminate MAI because of its inherent zero cross-correlation property. Moreover, this code's construction is notably straightforward. Regardless of its weight, its detection at the decoder only requires a single wavelength, making it less hardware-intensive compared to alternative codes. Another noticeable 2D spectral/spatial coding framework for OCDMA was introduced by Matem and colleagues in [7]. They used 2D-ZCC/MD code, however, the system hardware for 2D MD code was simpler than the 2D ZCC/MD code-based OCDMA system. Another recent work on 2D Spectral/spatial OCDMA systems was done by [10], where 2D-Balanced Incomplete Block Design (BIBD) code was utilized. However, this could support a data rate of up to 2.5 Gbps, beyond which the Bit Error Rate (BER) fell below 10^{-9} , leading to communication deterioration. A commonly accepted minimum BER for reliable telecommunication applications is 10^{-9} to 10^{-13} might be

necessary. There's no single "acceptable" range for SNR. However, a higher SNR generally translates to a lower BER. For example, Free Space Optical (FSO) communication systems might achieve a BER of 10^{-6} with an SNR of around 25 dB [11, 12, 13].

c. FSO

Two primary categories of optical communication include Optical Fiber Communication (OFC) and Free-Space Optical (FSO) communication. Optical fibers have significantly superseded copper wire-based communication in core networks due to their various benefits over electrical and Radio Frequency (RF) waveguides. However, optical fiber communication presents certain drawbacks related to the nonlinear refractive index of the core material, leading to phenomena like self-phase modulation (SPM), Four-Wave Mixing (FWM), and Cross-Phase Modulation (XPM). These limitations impact transmission rates and distances.

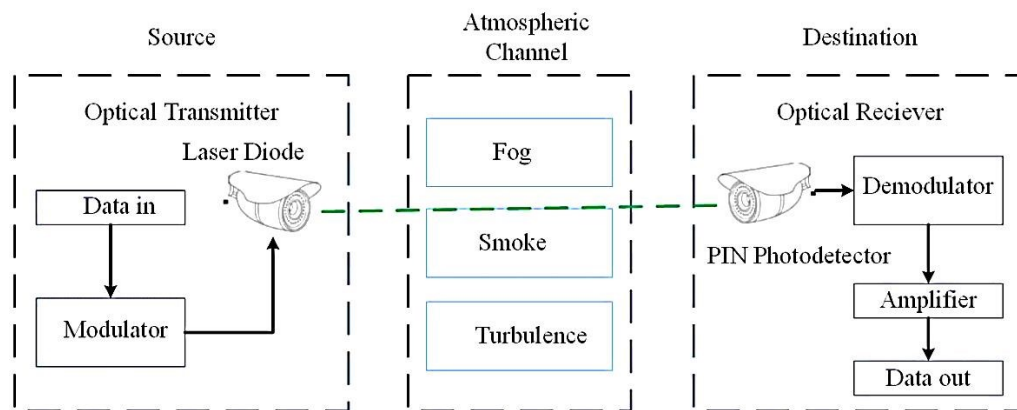


Fig. 2. FSO model Block Diagram

In contrast, Free-Space Optical (FSO) communication, also known as Free Space Photonics (FSP) or Optical Wireless, doesn't necessitate fiber use and can be deployed in metropolitan sites for inter-building communication. FSO communication involves transmitting modulated beams in the visible or infrared (IR) spectrum through the atmosphere to establish optical connectivity medium for telecommunication or computer networking purposes as shown in Fig. 2. FSO technology proves advantageous in scenarios where physical connections become impractical due to factors such as prohibitively high costs, deployment challenges, or other considerations. In recent times, FSO communication has garnered significant attention as a viable alternative to RF connections, particularly for swiftly transmitting data across short distances at elevated speeds, as highlighted by [14]. In a coastal setting, [15] conducted experimental studies on FSO links. FSO possesses several key attributes that render it highly appealing when compared to RF, microwave, and similar technologies. These include features like high data rates, utilization of unlicensed

spectrum, energy efficiency, cost-effectiveness, rapid deployment, and enhanced security. The performance of FSO channel highly depends on diverse weather conditions. There are different types of weather conditions (i.e., clean air, cloudy, foggy, rainy, stormy), and each of them poses a certain level of degradation in terms of signal attenuation on the FSO channel. These factors must be taken into account when working with FSO-based optical communication system. In [12], hybrid FSO based XG-PON is designed using Mode Division Multiplexing (MDM) techniques. In [13], a novel 120Gbps FSO system is presented which is utilizing three multiplexing techniques namely Orthogonal Frequency Division Multiplexing (OFDM) Polarization Division Multiplexing (PDM) and Optical Code Division Multiple Access (OCDMA).

d. XG-PON

XG-PON stands for 10-Gigabit-capable Passive Optical Network. It is a next-generation passive optical

networking technology that delivers data rates of up to 10 Gbps (gigabits per second) over a single fiber-optic line. XG-PON is an evolution of the previous generation GPON (Gigabit-capable Passive Optical Network) technology, which offered data rates up to 2.5 Gbps. XG-PON is designed to provide higher bandwidth and greater capacity, making it suitable for various applications that require high-speed and reliable internet connections. It can be used in residential, business, and enterprise environments to deliver ultra-fast internet services, support multimedia applications, and accommodate the increasing demand for bandwidth-intensive services like online gaming, high-quality video streaming, and cloud computing. This optical network is a cost-effective option in many ways including the fact that the splitters used in it are passive, i.e., they do not require power to work. Such optical networks combined with suitable multiplexing techniques and coding schemes can provide a simple yet robust and high data rate network that can fulfill the requirements of the modern era.

The effectiveness of an OCDMA-based system's performance is predominantly influenced by factors like MAI and PIIN, as detailed by [8]. OCDMA systems can be classified based on their coding strategies, which encompass both one-dimensional (1D) and hybrid code schemes.

Within the realm of 1D codes, they are further classified into Spectral Amplitude Coding (SAC), Temporal Coding, and Spatial Coding. Hybrid coding emerges when multiple coding techniques are amalgamated, as outlined in the work of [8]. Spectral Amplitude Coding involves partitioning the spectral bandwidth and segmenting the light source into discrete wavelengths. Spatial coding employs multiple fibers to generate code patterns, spatially distributing the code of each user across the fiber. While 1D codes offer commendable system performance, their primary limitation lies in the necessity for extended code length to facilitate multiple users, thereby demanding significant bandwidth. To address this challenge, Two-Dimensional (2D) codes have been introduced. These 2D codes are crafted by merging distinct 1D codes, such as Spectral-Time, Spectral-Spatial, and Spatial-Time, effectively tackling the issue of accommodating numerous users with shorter code lengths and lower bandwidth requirements. Yang and Huang's investigation revolved around spatial-spectral codes referred to as 2D *m*-matrices, with "*m*" representing the maximal area, as elucidated in their work in 2003 [16]. These codes were crafted using 1D *M*-sequences. C. H. Lin and team [17] introduced a set of codes by employing the 2D spatial-spectral methodology. Termed as 2-dimensional perfect difference (2D-PD) codes, this family of codes showcased the ability to diminish the impact of MAI and enhance the overall performance of the system.

A 2D code construction was formulated by combining two distinct codes: Modified Quadratic Congruence (MQC) code and *M*-sequence codes [18]. The MQC code was applied in the spectral domain, while the *M*-sequence code was employed in the spatial domain. These codes

were implemented utilizing tunable FBGs along with optical splitters and combiners. The analysis of code implementation accounted for receiver noise sources, including thermal shot, phase-induced intensity noise, and shot noise.

In [18], a comparative analysis was conducted between MQC-based codes and their counterpart *M*-matrix codes. The results substantiated the MQC-based codes' ability to concurrently accommodate a large number of users. Another contribution can be found in [17], where a 2D spectral-spatial code was introduced. The code known as 2D diluted perfect difference (DPD) code was derived from the 1D PD code and the dilution method.

A novel 2D Multi-Diagonal (2D-MD) code, was introduced and evaluated at both 1 Gbps and 2 Gbps data rates by [8]. This code was established upon a foundation of a 1D-MD code [9], which found application within the spectral and spatial domains. The standout attribute of the 2D-MD codes is their ability to exhibit zero-cross correlation. This unique property facilitates the effective mitigation of PIIN and MAI within the optical system. Through a comparative analysis, the author contrasted the performance of the 2D-MD code with that of the 1D MD code, 2D-PD code, and 2D-DPD codes. The study's conclusion pointed towards the superior performance of the two-dimensional MD code when compared to the other code variants. This assertion was supported by the results obtained through both simulation and analytical methods, ultimately highlighting the versatility and effectiveness of the proposed 2D-MD code.

Cherifi et al. in [19], proposed a two-dimensional code derived from the Single Weight Zero Cross-Correlation (SWZCC) code, initially proposed by Malleswari and Murugesan in [20]. This code type was recognized for its ability to maintain zero cross-correlation and conferred the advantageous ability to efficiently accommodate a substantial number of users. Through numerical simulations, the researchers demonstrated the efficacy of this code by considering a scenario involving four users transmitting at a power of -10 dBm with a data rate of 1 Gbps. The findings underscore the substantial improvement in network capabilities achieved by this code, coupled with a concurrent reduction in the required Signal-to-Noise Ratio (SNR).

In the study carried out by Tseng et al. [21], the researchers proposed a set of codes referred to as extended *M*-sequence/extended perfect difference (EMS/EPD) codes. These codes were developed specifically for application in 2D spectral-spatial OCDMA PON systems.

In the study conducted by Matem et al. [7], a unique hybrid code referred to as 2D ZCC-MD was proposed for implementation in spectral-spatial OCDMA systems. The performance of this code was assessed in a 622 Mbps OCDMA system and performance was compared with 1 dimensional RD and MDW codes. The findings highlighted that the 2D ZCC-MD code family can effectively support a substantial number of users at high data rates.

A 2D Enhanced Multi-Diagonal (2D-EMD) code was introduced for utilization in OCDMA-PON systems [22].

The study involved an analysis of the 2D EMD code and its comparison with alternative codes, leading to the conclusion that it is well-suited for enabling next-generation PONs operating at both 622 Mbps and 1 Gbps.

In the research by [23], a 2D wavelength/time encoding code was presented as a solution to minimize MAI. The proposed code employed 2D Modified Double-Photon Hadamard Code (2D MDPHC) at a rate of 1.25 Gbps. An alternative approach, introduced by [24], outlined an algorithm termed the two-dimensional fixed right shifting (2D-FRS) code sequences. This algorithm was designed for a spectral-spatial incoherent OCDMA system. Another contribution came from [25], who proposed a method for generating a 2D optical Zero-Correlation Zone (ZCZ) sequence. In the study conducted by [26], simulations were performed to assess the performance of the system across different lengths of optical fiber. This evaluation took place within a 2D single-user OCDMA-PON system, and the system's architecture was built upon cascaded FBGs.

Moreover, MD codes demonstrated enhanced performance across metrics such as Bit Error Rate (BER), spectral efficiency, higher bit rates, and the capacity to accommodate a greater number of simultaneous users, as evidenced by the research of [27]. In a separate study, [28] introduced and examined a 2D cyclic shift (2D-CS) code,

comparing its effectiveness against several alternative 2D codes over a distance of 20 kilometers using Single-Mode Fiber (SMF). [29] designed GPON based on 2D MD code. The authors analyzed the performance at data rates from 622 mbps to 15 Gbps.

A significant portion of the available research has put forward innovative algorithms to augment the capacity of a fundamental OCDMA system, particularly concentrating on data rates of up to 1.25 Gbps.

2. Proposed system

2.1. Proposed system architecture

The proposed work is undertaken to realize the implementation of a 2D spectral/spatial coding framework for OCDMA in PON. This framework is intended to enhance the overall system performance of the OCDMA network in comparison to the 1D code framework. The proposed work also utilizes the FSO channel in the last-mile network. The system block diagram is shown in Fig. 3, it consists of 5 major parts, namely Optical Line Terminal (OLT), the backbone Single Mode Optical Fiber Cables, the Remote Nodes (RN), The Free Space Optical channels (FSO), and the Optical Network Unit (ONU).

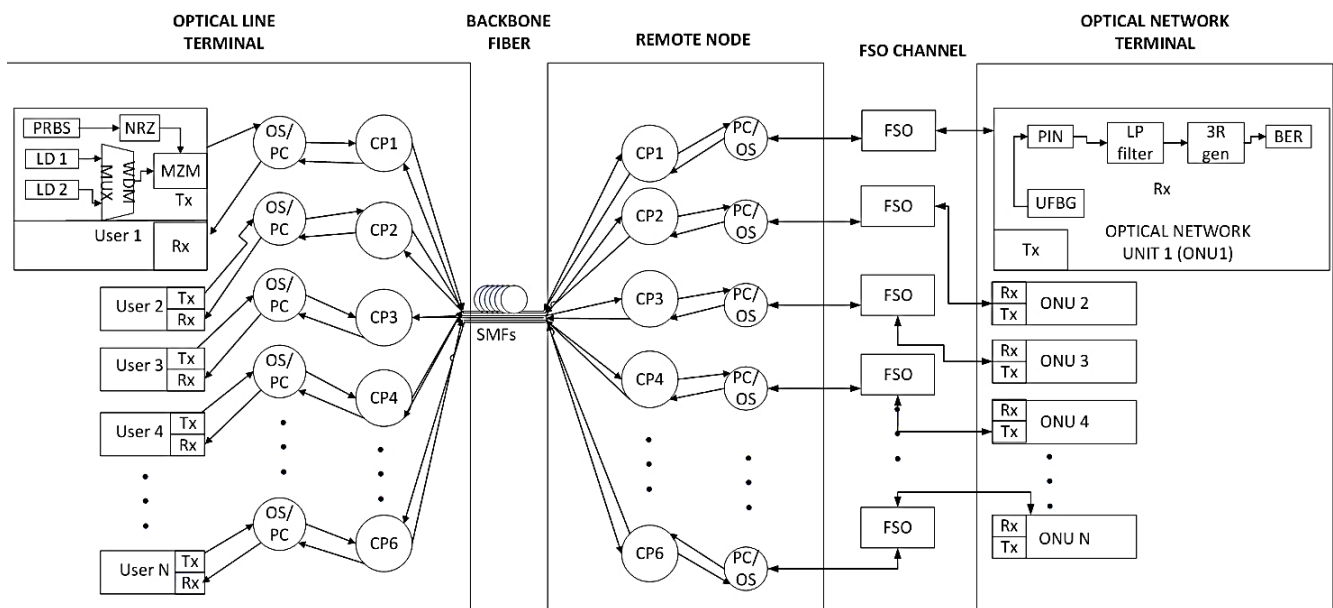


Fig. 3. Proposed system block diagram (color online)

The OLT is considered as a central office, and the ONUs are the users connected to the optical network. As this is a full-duplex system, both OLT and ONU consist of transceivers based on 2D-MD OCDMA codes. The 2D coding is done using spectral and spatial dimensions, by assigning unique MD codes to each user for spectral coding and utilizing multiple SMF cables for spatial

coding. The couplers and power splitters are used in the architectural design to achieve 2D coding [29].

The transmitter part of the transceiver consists of Continuous Wave (CW) laser source, a Pseudo Random Bit Sequence Generator (PRBS), a multiplexer, a Mach-Zehnder Modulator (MZM), and a Non-Return to Zero (NRZ) pulse generator. The transmitter section is shown in Fig. 4. Every user is assigned a unique code and based on

that a specific wavelength is assigned to each user's CW laser. Laser sources have a longer range and can provide better performance than LEDs. Input from the light source is modulated via PRBS in the MZM. NRZ is used as a line coding technique to carry the user data generated by PRBS. Each user has its own code-word which is known to its respective receiver. The MZM output is given to the

splitters that will split the signal depending on the weight of the code sequence. This data is then spatially divided and transmitted over Single-Mode Fiber (SMF) cable to the ONUs. At the ONU, the last mile network consists of another transceiver that decodes the incoming signal based on its intended wavelength.

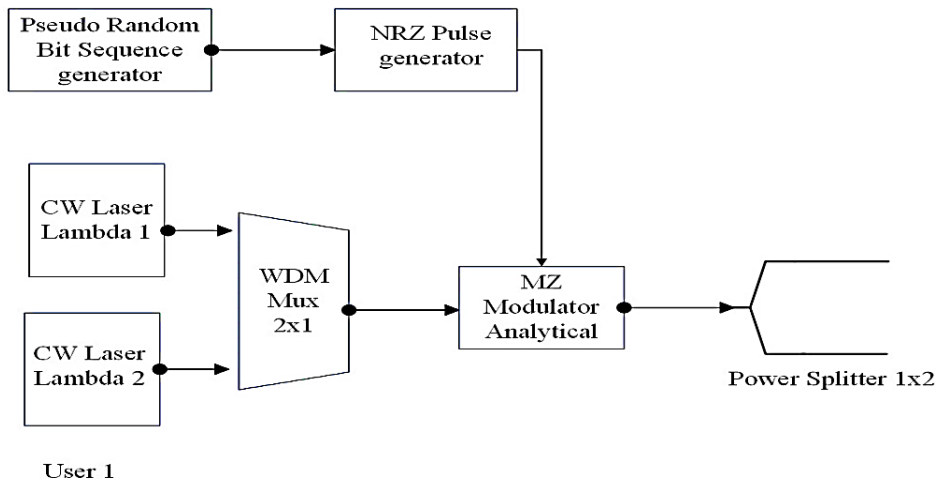


Fig. 4. Transmitter design model of proposed system

The receiver part of the transceiver, shown in Fig. 5, consists of decoding process based on Uniform Fiber Bragg Gratings (UFBG), PIN photodiode, a Low pass Filter, and the 3R generator. The FBG is responsible for detecting the spectral code of each user and that light signal is then sensed by photodiode and converted to

electrical signal which is passed through LP filter toward 3R regenerator for strengthening the signal. Notice that due to the simplicity of MD code, just one FBG is required per user in this network design, making it less complicated [29].

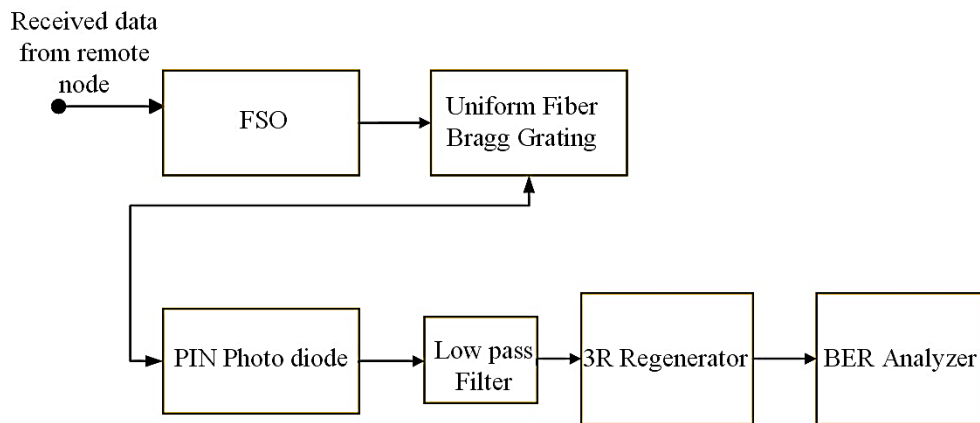


Fig. 5. Receiver design model of proposed system

FSO channel is introduced at the ONUs. The optical data arriving at the user end reaches the last mile network via FSO channel which replaces the copper cable from the optical network making it all-optical. Due to this change, a huge difference is noticed in the data rate. The parameters to be considered for the FSO channel are included in the mathematical analysis of this proposed system. Weather conditions, i.e., rain and haze, are taken into consideration. FSO channel parameters, rain and haze attenuation levels are taken from [30]. 2D-OCDMA and FSO in the last

mile, both technologies, when combined, will provide data rate in Gbps with acceptable SNR and BER for the XG-PON.

2.2. Pseudo algorithm

The algorithm for the proposed system mathematical model is presented in the following Table 1.

Table. 1. Pseudo algorithm for proposed methodology

ALGORITHM FOR MATHEMATICAL MODEL OF 2-DIMENSIONAL MULTI-DIAGONAL CODE WITH FSO WEATHER CONDITIONS	
Responsivity Calculation:	<p>Input Parameters</p> <p>qq1 = 0.6 // Quantum efficiency h = 6.66×10^{-34} // Planck constant f = $3 \times 10^8 / 1.55 \times 10^{-6}$ // Optical frequency ee1 = 1.602×10^{-19} // Charge on electron</p> <p>Output Equation</p> <p>R = (qq1 * ee1) / (h * f) // Responsivity</p>
Variance Calculation:	<p>Input Parameters</p> <p>Tc = 1.00×10^{-10} // Chip duration Ib = 0.1×10^{-9} // Background current Is = 10×10^{-9} // Surface leakage current Kb = 1.379×10^{-23} // Boltzmann's constant RL = 1030 // Load resistance Tr = 300 // Receiver temperature B = 311×10^6 // Bandwidth of receiver</p> <p>Output Equation</p> <p>th = (4 * Kb * Tr * B) / (RL) // Variance of thermal noise</p>
Beta Rain Scattering:	<p>Input Parameters</p> <p>Qscat = 2 lambda = 1550×10^{-9} a = 0.001 // Radius of raindrop (0.001-0.1cm) pi = 3.14</p> <p>Output Parameters</p> <p>V = (2 * a² * 1 * 980) / (9 * 1.8 * 10⁻¹⁴) Na = 3 * (2.22 * 10⁻³) / (4 * (pi * a³) * V)</p> <p>Output Equation</p> <p>$\beta_{rain} = pi * a^2 * Na * Qscat * (a / lambda)$</p>
Rain attenuation using Beer's law:	<p>Input Parameters</p> <p>R = 500</p> <p>Output Equation</p> <p>T = exp(-$\beta_{rain} * R$)</p>
Beta haze scattering:	<p>Input Parameters</p> <p>visibilty = 49×10^5 // Beta haze scattering high visibility in m q_scatter = 1.6 // Size distribution of scattering particles</p> <p>Output Equations</p> <p>x = (lambda / 550×10^{-9})^(-q_scatter) $\beta_{haze} = (3.91 / visibilty) * x$</p>
BER Calculation:	<p>Input Parameters</p> <p>dv = 6.25×10^{12} // Linewidth of light source P1 = -10 // Power in dBm Psr1 = 0.001 * 10^(P1/10) // Power in Watts dv = 6.25×10^{12} // Bandwidth of light source N = 10 // Length of the codeword w1 = 2 k2 = 3 k1 = 4 K = k1 * k2 // Total active users</p> <p>Initialize SNR6 as an empty array</p> <p>Loop for K from 1 to 130 for K = 1 to 130 a. num1 = (R * Psr1 * k2 / K)² b. den1 = (ee1 * B * R * Psr1 * k2 / K) + th + β_{rain} // for rain c. snrb = num1 / den1 d. Append SNR6 = [SNR6 snrb] End for loop</p>
Output	<p>BER1 = 0.5 * q(sqrt(SNR6 / 8)) SNR6</p>
End	

2.3. Mathematical model

During the analysis of proposed 2D-MD-based system, the noise components encompass thermal noise, shot noise, and atmospheric noise. The property of zero cross-correlation exhibited by MD codes eliminates spectral overlap among different users, rendering the MAI noise negligible. For the analysis, the influence of the receiver's dark current is presumed to be negligible. To calculate the bit error rate (BER), the Gaussian approximation method is employed, as outlined in the work by [9]. This approach takes into account thermal noise and shot noise within the photo-detector, as well as atmospheric noise stemming from the free-space optical channel in the last-mile network.

$$\sigma_{\text{noise}}^2 = \langle i_{\text{shot}}^2 \rangle + \langle i_{\text{thermal}}^2 \rangle + \langle i_{\text{atmospheric_noise}}^2 \rangle \quad (1)$$

where,

$$\langle i_{\text{shot}}^2 \rangle = 2eBI \quad (2)$$

$$\langle i_{\text{thermal}}^2 \rangle = \frac{4K_b T_n B}{R_L} \quad (3)$$

$$\langle i_{\text{atmospheric_noise}}^2 \rangle = \beta_{\text{rain_scat}} + \beta_{\text{haze}} \quad (4)$$

$$\beta_{\text{rain_scat}} = \pi a^2 N a Q_{\text{scat}} \left(\frac{a}{\lambda} \right) \quad [31] \quad (5)$$

$$\beta_{\text{haze}} = \frac{3.91}{V} \left(\frac{\lambda}{550 \text{ nm}} \right)^{-q} \quad [31] \quad (6)$$

Putting Eq. (2), (3), and (4) in Eq. (1), it becomes:

$$\sigma^2 = 2eBI + \frac{4K_b T_n B}{R_L} + \beta_{\text{rain_scat}} + \beta_{\text{haze}} \quad (7)$$

The power spectral density of the received optical signals can be represented as [29]:

$$r(v) = \frac{P_{sr}}{W_2 \Delta v} \sum_{k=1}^K d_k \sum_{j=0}^{P-1} \sum_{i=0}^{M-1} a_{(i,j)}(k) \text{rect}(i) \quad (8)$$

where P_{sr} is the effective power, d_k is the data bit of k th user.

Using the $\text{rect}(i)$ function given in Eq. (9).

$$\text{rect}(i) = u \left[v - v_0 - \frac{\Delta v}{2N} (-N + 2i - 2) \right] - u \left[v - v_0 - \frac{\Delta v}{2N} (-N + 2i) \right] \quad (9)$$

$$\text{rect}(i) = u \left[\frac{\Delta v}{N} \right] \quad (10)$$

where $u(v)$ is the unit step function expressed as:

$$u(v) = \begin{cases} 1, & v \geq 0 \\ 0, & v < 0 \end{cases} \quad (11)$$

The integral of $G(v)$, is the integration of the power spectral density at the photo-detector of the l th receiver during one period and can be written as:

$$\int_0^\infty G(v) dv = \int_0^\infty \left[\frac{P_{sr}}{\Delta v} \sum_{k=1}^K d_k \sum_{i=1}^N c_k(i) \text{rect}(i) \right] dv \quad (12)$$

The above equation can be simplified using the correlation properties of MD code as following:

$$\int_0^\infty G(v) dv = \frac{P_{sr}}{\Delta v} \left[\sum_{k=1}^K d_k W \frac{\Delta v}{N} + \sum_{k=1}^K d_k 0 \frac{\Delta v}{N} \right] \quad (13)$$

$$\int_0^\infty G(v) dv = \frac{P_{sr}}{\Delta v} \left[\sum_{k=1}^K d_k W \frac{\Delta v}{N} \right] \quad (14)$$

where, d_k is the data bit (either be 0 or 1). Assuming all users are transmitting data bit 1, then:

$$\left[\sum_{k=1}^K d_k \right] = [d_1 + d_2 + d_3 + \dots + d_{K-1} + d_K] = W \quad (15)$$

Consequently,

$$\int_0^\infty G(v) dv = \frac{P_{sr}}{\Delta v} \left[W \frac{\Delta v}{N} \cdot \sum_{k=1}^K d_k \right] = \frac{P_{sr}}{\Delta v} \left[W \frac{\Delta v}{N} \cdot W \right] = \frac{W^2 P_{sr}}{N} \quad (16)$$

The cross-correlation between $A_{0,0}^0$ and $A_{g,h}$ can be calculated as:

$$I = \Re \int_0^\infty G(v) dv \quad (17)$$

$$I = \Re \int_0^\infty \frac{P_{sr}}{W_2 \Delta v} \sum_{k=1}^K d_k R^0(i, j) \text{rect}(i) dv \quad (18)$$

$$I = \Re \frac{P_{sr} \Delta v}{W_2 \Delta v M} \left[W_1 W_2 + \sum_{k=2}^K d_k R^0(i, j) \right] \quad (19)$$

$$I = \frac{\Re P_{sr} \Delta v}{W_2 \Delta v M} [W_1 W_2 + 0] \quad (20)$$

$$I = \frac{\Re P_{sr} W_1}{M} \quad (21)$$

where, I is the photocurrent, $\Re = (\eta e)/hf$ is the responsivity of the photodetectors [30], h is Planck's constant, η is the quantum efficiency, and f is the central frequency of the original broadband optical pulse.

Putting $M = W_1 K_1$ and $K = K_1 K_2$, we get:

$$I = \frac{\Re P_{sr} K_2}{K} \quad (22)$$

Now, substitute Eq. (21) and Eq. (5),

$$\sigma^2 = 2eB \Re \frac{P_{sr} K_2}{K} + \frac{4K_b T_n B}{R_L} + \beta_{\text{rain_scat}} + \beta_{\text{haze}} \quad (23)$$

The probability of sending data bit 1 is 50%, hence the above Eq.(13) becomes:

$$\sigma^2 = \frac{eB\mathfrak{R}P_{sr}K_2}{K} + \frac{4K_bT_nB}{R_L} + \beta_{rain_{scat}} + \beta_{haze} \quad (24)$$

The average Signal to Noise Ratio can be calculated as:

$$SNR = \left[\frac{\left(\frac{\mathfrak{R}P_{sr}K_2}{K} \right)^2}{\frac{eB\mathfrak{R}P_{sr}K_2}{K} + \frac{4K_bT_nB}{R_L} + \beta_{rain_{scat}} + \beta_{haze}} \right] \quad (25)$$

The Bit Error Rate can be calculated by using Gaussian approximation:

$$BER = \frac{1}{2} \operatorname{erfc} \left(\sqrt{\frac{SNR}{8}} \right) \quad (26)$$

where,

$$\operatorname{erfc}(z) = \frac{2}{\sqrt{\pi}} \int_z^{\infty} e^{-y^2} dy \quad (27)$$

Based on the mathematical analysis described above, the subsequent graphs are assessed, effectively confirming the accuracy of the simulation outcomes. The specific parameters employed in the analytical calculations can be found in Table 2.

Table 2. Parameter values for mathematical analysis

Symbol	Parameter	Value
\mathfrak{R}	Photodetector responsivity	0.75
T_n	Temperature of the receiver noise	300 K
R_L	load resistor of the receiver	1030 Ohms
P_{sr}	effective power	-10 dBm

3. Results and discussions

The two parameters BER and SNR are used to analyze the performance of the proposed system under different weather conditions. Weather conditions are necessary to take into consideration because we are using FSO channel in the last mile whose performance greatly varies with respect to the type of weather. The mathematical model is used to generate these graphs using MATLAB software.

For analyzing FSO channel performance in 2D-OCDMA based XG-PON various weather conditions are considered, e.g., heavy rain, medium rain, light Rain, and Hazy weather. Our mathematical analysis based on the Kim and Kruse model for hazy weather and Stoke's scattering law for rain scattering [31] provides the following results:

Fig. 6a provides the BER curve with respect to number of active users. This curve is generated for the FSO channel in 2D-OCDMA based XG-PON being analyzed during heavy rainy weather. As shown in this figure, 22 active users have BER of 2.65457×10^{-9} . This means that the proposed system will provide an acceptable performance even in extreme weather conditions.

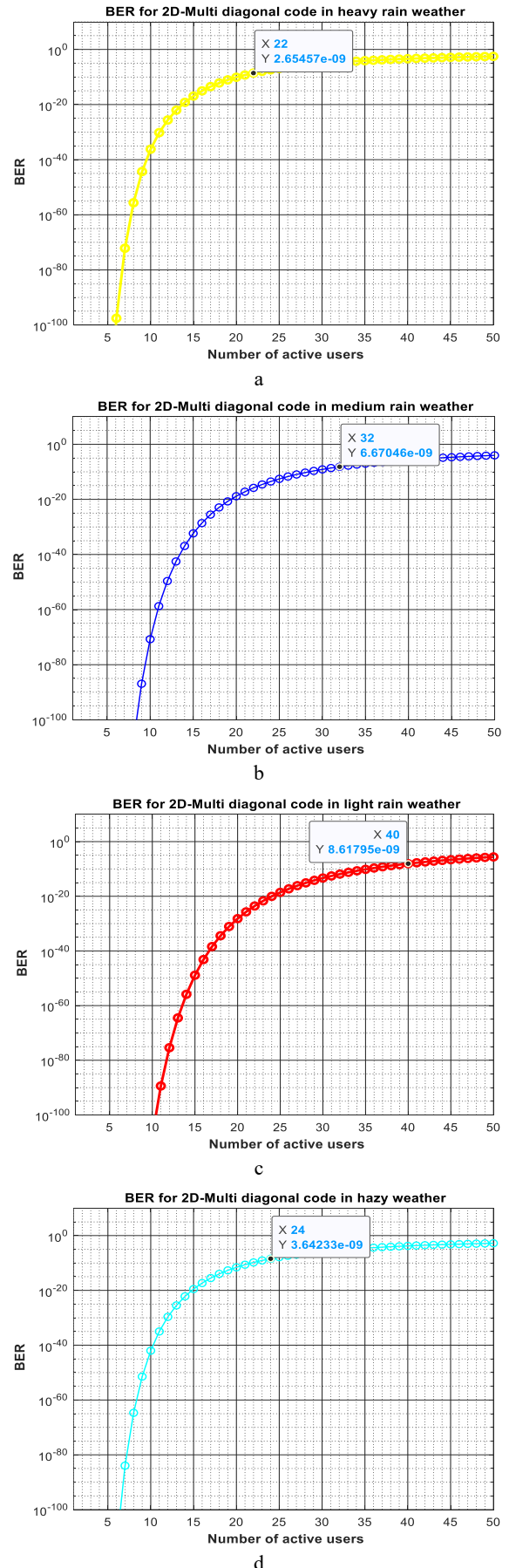


Fig. 6. BER for proposed system under (a) heavy rain (b) medium rain (c) light rain (d) under haze (color online)

The response of the proposed system is again tested for medium rainy weather. The BER curve with respect to number of active users for medium rainy weather in the proposed system is given in Fig. 6b. This curve provides a better performance of the proposed system in comparison to the heavy rain weather shown in Fig. 6a. The number of active users has increased to 32 at 6.67046×10^{-9} .

Improvement in number of active users is evident since the start and it can be seen that if users are in the range of 5 to 20 the BER is in the order of 10^{-20} or less which means the proposed system will be able to provide high quality service even in bad weather.

Fig. 6c shows the BER curve during light rain with a much better performance by achieving 40 simultaneous active users. BER rate is 8.61795×10^{-9} and this proves that the proposed system if installed in the clear weather will provide a seamlessly very high data rate of huge number of active users. Finally, in Fig. 6d the BER curve provided is for hazy weather. This curve shows that 24 users can be accommodated at 3.64233×10^{-9} . An important point here to be observed is that haze is more deteriorating the signal transmission after heavy rain, because in haze the particles stay in the air for longer time as compared to rain.

Signal to Noise Ratio (SNR) is another important parameter that measures the quality of signal transmission. SNR provides the signal performance in the presence of noise in the communication network. Having as high SNR ensures that the signal strength is higher than noise and hence the system is reliable.

As shown in Fig. 7a to 7d, SNR graphs depict the signal strength of the proposed system in heavy rain, medium rain, light rain, and haze. SNR in all these weather conditions is acceptable as shown in their respective figures.

A typical passive optical network works on 1510 nm wavelength for downstream communication and 1310 nm wavelength for upstream communication. Fig. 8 depicts the comparison of the proposed system model at different wavelengths. 1550 nm, 1310 nm and 785 nm wavelengths are compared and the number of users working synchronously on 1550 nm is the highest. This supports the system robustness in terms of the typical wavelengths. It must also be noted that at 1310 nm the proposed system provides similar performance as compared to 1510 nm wavelength. Hence the overall results are promising.

Table 3 below points out the comparison between previous works and proposed work. It must be noted that the proposed works' BER, SNR, over all capacity, all are better as compared to previous works. Also, the number of channels is 22 for heavy rain, 32 for medium rain, 40 for light rain, and 24 under hazy weather. And regardless of weather condition the overall SNR is > 100 . This can be seen in Figs. 7a to 7d as well.

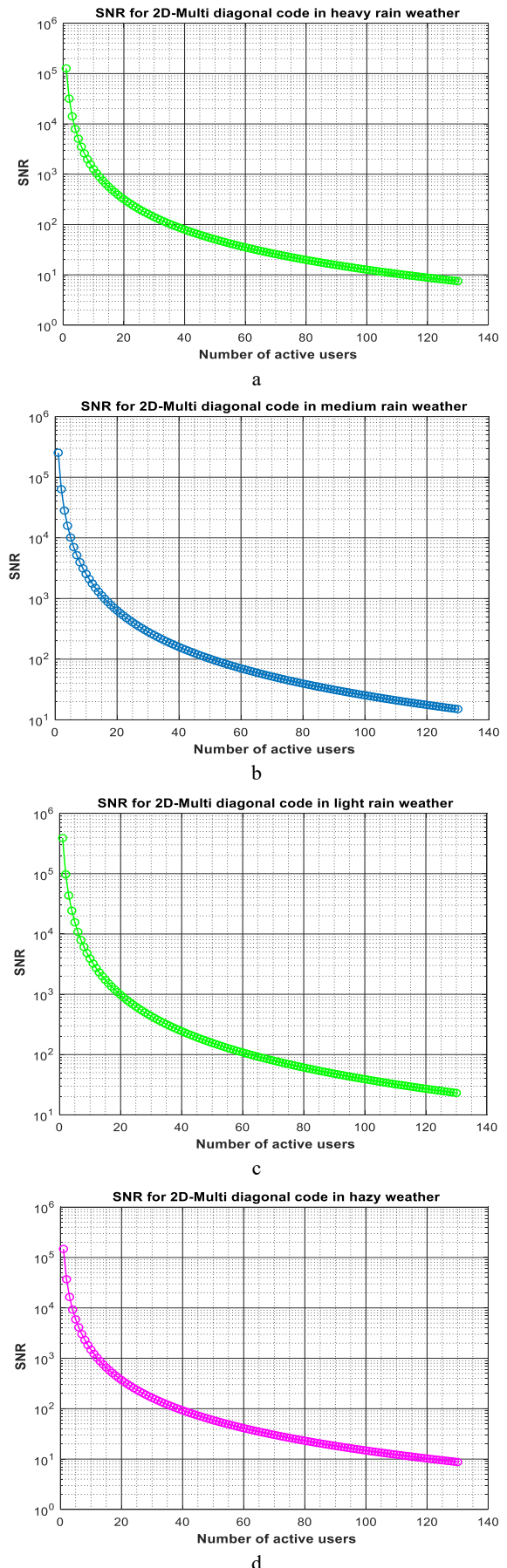


Fig. 7. SNR for proposed system under (a) heavy rain (b) medium rain (c) light rain (d) under haze (color online)

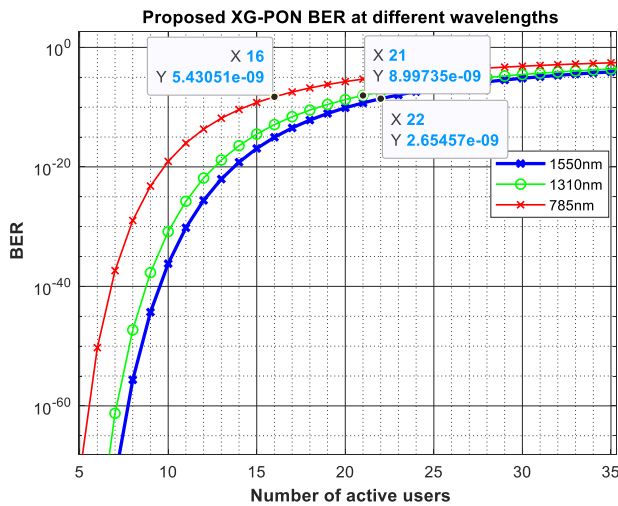


Fig. 8. Proposed System BER at different wavelengths (color online)

4. Conclusion

In this paper, next-generation passive optical network design is proposed based on popular 2D-Multi-diagonal OCDMA code along with free space optical channel in the last-mile network. The performance of this proposed

system is analyzed using its mathematical model where effects of thermal noise and shot noise along with weather conditions like rain and haze are considered which are crucial if FSO channel is implemented. Based on the BER and SNR curves achieved from the numerical analysis, the performance of the 2D-OCDMA based XG-PON using FSO in last mile gives a good performance with improved number of active users. Furthermore, it can be seen from Fig. 8 that the proposed system is suitable for uplink as well as downlink optical network. The proposed system provides high data rates and improved performance, making it suitable for delivering essential services like health information, education, e-government, and agriculture to rural areas. It combines the resilience of fiber optics with the cost efficiency of FSO, making it adaptable to various deployment scenarios. The proposed system could serve as an alternative communication network, ensuring connectivity even when other systems are disrupted. FSO technology is often used in military applications due to its security and immunity to electromagnetic interference. The proposed hybrid system could enhance military communication networks, especially in challenging terrains or remote locations. The proposed system could support smart city initiatives, connecting sensors, surveillance cameras, and other IoT devices seamlessly.

Table 3. Comparison of proposed work with previous work

References	Multiplexing Technique	Transmission	Number of channels	SNR	BER	Weather condition	Overall Capacity
T. Sharma, et al. (2021) [10]	OCDMA 2D BIBD codes	Not given	6	better	10^{-9}	Not included	2.5 Gbps
H. Mrabet, et al. (2021) [27]	IM/DD Fast-OFDM-CDMA	Bidirectional	4	Not given	$10^{-4.5}$	Not included	40 Gbps
K. A. Memon, et al. (2022) [30]	OCDMA using MD code	Bidirectional	5	Not given	10^{-11}	Clear air, haze, rain	100 Gbps
M. Kumari, et al. (2024) [12]	Mode Division Multiplexing (MDM)	Bidirectional	4	42	10^{-9}	Clear air, haze, rain	10 Gbps
El-Mottaleb, et al. (2024) [13]	OFDM, PDM, OCDMA using ICSM code	Not given	6	Not given	10^{-3}	Haze, rain, and fog	120 Gbps
Proposed work	OCDMA 2D MD codes	Bidirectional	22,32,40,24	>100	10^{-9}	Heavy rain, medium rain, light rain, haze	10 Gbps x 40 (# of channels) = 400Gbps

References

- [1] N. Karafolas, D. Uttamchandani, *Opt. Fiber. Tech.* **2**(2), 149 (1996).
- [2] H. W. Chen, G. C. Yang, C. Y. Chang, T. C. Lin, W. C. Kwong, *J. Lightwave Technol.* **27**(14), 2771 (2009).
- [3] S. Kaur, S. Singh, *Opt. Eng.* **57**(11), 116102 (2018).
- [4] E. Faleet, S. Saber, Thesis, The Islamic University, Gaza, 2015.
- [5] H. Yin, D. J. Richardson, "Optical code division multiple access communication networks: Theory and applications," Springer Berlin, Heidelberg, 1–382, 2009.
- [6] R. A. Kadhim, H. A. Fadhil, S. A. Aljunid, M. S. Razalli, 4th IEEE International Conference on Control System, Computing and Engineering, ICCSCE 2014. (pp. 90–94).
- [7] R. Matem, S. A. Aljunid, M. N. Junita, C. B. M. Rashidi, I. S. Aqrab, *Indonesian J. of Electrical Eng. and Comp. Science* **14**(2), 661 (2019).
- [8] R. A. Kadhim, H. A. Fadhil, S. A. Aljunid, M. S. Razalli, *Opt. Commun.* **329**, 28 (2014).
- [9] T. H. Abd, S. A. Aljunid, H. A. Fadhil, R. A. Ahmad, N. M. Saad, *Opt. Fiber Tech.* **17**(4), 273 (2011).
- [10] T. Sharma, A. Chehri, P. Fortier, H. Yousif Ahmed, M. Zeghid, W. A. Imtiaz, *Applied Sciences* **11**(2), 1 (2021).
- [11] Menna Taher, Mohamed Abaza, Mostafa Fedawy, Moustafa Aly, *App. Sci.* **9**(7), 1281 (2019).
- [12] M. Kumari, V. Arya, "Four Laguerre–Gaussian mode division multiplexed incorporated hybrid XG-PON and FSO Gamma fading system under severe weather conditions" Springer Berlin, Heidelberg, 113, 2024.
- [13] S. A. A. El-Mottaleb, M. Singh, M. H. Aly, "120 Gbps FSO transmission system based on integrated OFDM-PDM-OCDMA transmission using ICSM code: performance analysis" Springer Berlin, Heidelberg, 621, 2024.
- [14] A. K. M. N. Islam, S. P. Majumder, In 18th International Conference on Computer and Information Technology, ICCIT pp. 341–346, 2015.
- [15] Wael G. Alheadary, Ki-Hong Park, Nasir Alfaraj, Yujian Guo, Edgars Stegenburgs, Tien Khee Ng, Boon S. Ooi, Mohamed-Slim Alouini, *Opt. Express*, **26**(6), 6614 (2018).
- [16] C. C. Yang, J. F. Huang, *IEEE Photonics Tech. Lett.* **15**(1), 168 (2003).
- [17] B. C. Yeh, C. H. Lin, J. Wu, *J. Opt. Comm. Netw.* **2**(9), 653 (2010).
- [18] C. C. Yang, J. F. Huang, I. M. Chiu, *IEEE T. Commun.* **55**(1), 40 (2007).
- [19] A. Cherifi, N. Jellali, M. Najjar, S. A. Aljunid, B. S. Bouazza, *Opt. Laser Tech.* **109**, 233 (2019).
- [20] M. Malleswari, K. Murugesan, *Journal of Optics* **42**(4), 307 (2013).
- [21] S. P. Tseng, J. Wu, W. H. Yang, *IEEE T. Commun.* **60**(11), 3451 (2012).
- [22] W. A. Imtiaz, H. Y. Ahmed, M. Zeghid, Y. Sharief, M. Usman, *Arabian Journal for Science and Engineering* **44**(8), 7067 (2019).
- [23] S. Panda, G. Palai, *Optik* **207**, 163864 (2020).
- [24] H. Y. Ahmed, M. Zeghid, W. A. Imtiaz, A. Sghaier, *Opt. Fiber Tech.* **47**, 73 (2019).
- [25] T. Matsumoto, H. Torii, Y. Ida, S. Matsufuji, International Symposium on Intelligent Signal Processing and Communication Systems, ISPACS pp. 1 – 2, 2019.
- [26] M. Zheng, Q. Wu, Y. Zhou, L. Jiang, J. Liu, *J. Physics, Conf. Ser.* **2113**(1), 01207 (2021).
- [27] H. Mrabet, A. Cherifi, T. Raddo, I. Dayoub, S. Haxha, *IEEE Syst. J.* **15**(3), 3642 (2021).
- [28] M. Alayedi, A. Cherifi, A. Ferhat Hamida, H. Mrabet, *Telecom. Syst.* **79**(2), 193 (2022).
- [29] K. A. Memon, A. Atieh, A. W. Umrani, M. A. Unar, W. Shah, *Opt. Eng.* **59**(7), 076105 (2020).
- [30] K. A. Memon, A. W. Umrani, M. A. Unar, W. Shah, F. A. Umrani, *Wirel. Pers. Comm.* **126**(4), 3147 (2022).
- [31] H. A. Fadhil, A. Amphawan, H. A. B. Shamsuddin, T. H. Abd, H. M. R. Al-Khafaji, S. A. Aljunid, N. Ahmed, *Optik* **124**(19), 3969 (2013).

*Corresponding author: kehkashan@faculty.muet.edu.pk